MJFAS
Malaysian Journal of Fundamental and Applied Sciences

Permatasari *et al.* | Malaysian Journal of Fundamental and Applied Sciences, Vol. 22 (2026) 497-516

RESEARCH ARTICLE

In Vitro and In Silico Study of the Anticancer Activity of Benalu batu (*Begonia medicinalis* Ardi & D.C. Thomas) an Endemic Plant of Sulawesi Against A549 Lung Cancer Cells

Ni Kadek Dewi Permatasari, Rarastoeti Pratiwi*

Department of Biology, Faculty of Biology, Universitas Gadjah Mada, Yogyakarta, 55281, Indonesia

Abstract Lung cancer is one the leading causes of cancer related deaths worldwide. Standard therapies such as cisplatin are commonly used however, their long-term use can lead toxic effects on normal cells. Consequently, the search for alternative herbal based therapies has gained increasing attention. One potential candidate is Benalu batu (*Begonia medicinalis*), an endemic plant from Sulawesi that has been traditionally used as remedy for various ailments, including tumors and cancer. This study aims to evaluate the anticancer potential of ethanolic extract and fraction of Benalu batu both in vitro A549 lung cancer cells and Vero cells, and in silico against EGFR-TK and Bcl-2 proteins, which are involved in the progression of Non-Small Cell Lung Cancer (NSCLC). Cytotoxicity was assessed using the MTT assay, while compound identification was performed using Thin Layer Chromatography (TLC) and Gas Chromatography-Mass Spectrometry (GC-MS). Druglikeness feasibility was evaluated through Lipinski's Rule of Five using SwissADME, and molecular docking studies were conducted using PyRx and Visualized with Discovery Studio. The results demonstrated that the ethanolic extract of wild Benalu batu exhibited higher cytotoxic activity compared to the cultivated plant extract, with an IC_{50} value of 134.71 µg/mL, and was nontoxic to Vero cells (IC_{50} = 517.24 µg/mL). Thin Layer Chromatography profiling indicated that the compounds in the wild Benalu batu extract are predominantly non-polar. Cytotoxicity testing of the active fractions revealed that fraction A exhibited the most potent activity with an IC_{50} of 33.93 µg/mL and high selectivity index of 24.52, surpassing that of cisplatin. Gas Chromatography-Mass Spectrometry analysis identified eight bioactive compounds suspected to have anticancer potential, these compounds are stigmasterol (19.80%), campesterol (7.06%), neophytadiene (4.83%), sitosterol (3.29%), squalene (2.73%), phytol (2.39%), phytol acetate (1.22%), hexadecenoic acid ethyl ester (1.22%), and α-tocopheryl acetate (1.10%). Molecular docking against the EGFR-TK protein showed that campesterol (-9.2 kcal/mol), stigmasterol ((-9.1 kcal/mol), and sitosterol (-8.2 kcal/mol), had more favorable binding affinity values compared to the control drug gefitinib (-7.7 kcal/mol). Sitosterol exhibited the highest binding affinity (-8.7 kcal/mol) against Bcl-2 protein, followed by squalene and stigmasterol (-8.5 kcal/mol), and campesterol (-8.4 kcal/mol).

Keywords: *Begonia medicinalis*, anticancer, GC-MS, A549 cells, molecular docking.

***For correspondence:**
rarastp@ugm.ac.id

Received: 28 July 2025
Accepted: 28 March 2026

Introduction

Lung cancer remains one of the leading causes of cancer related mortality worldwide. According to GLOBOCAN 2022, there were approximately 2,480,675 new cases and 1,817,469 deaths attributed to lung cancer globally. Around 85% of these cases are categorized as Non-Small Cell Lung Cancer (NSCLC) [1]. The development of NSCLC is characterized by various molecular alterations, including the overexpression of the epidermal growth factor receptor (EGFR) [2]. EGFR is a transmembrane tyrosine kinase receptor that plays a crucial role in regulating cell proliferation, differentiation, and survival. Its activation induces autophosphorylation of the tyrosine kinase domain (EGFR-TK) and triggers various intracellular signaling pathways, such as Ras/Raf/MAPK and P13K/Akt/Mtor, promoting

uncontrolled cell growth and NSCLC progression [3] . In addition, NSCLC evades programmed cell death through the expression of the anti-apoptotic protein B-cell lymphoma-2 (Bcl-2). This protein regulates mitochondrial membrane permeability by inhibiting the activation of pro-apoptotic proteins such as BAX and BAK. This inhibition prevents the release of cytochrome c from the mitochondria into the cytosol, thereby suppressing the activation of caspases required to initiate programmed cell death [4]. Therefore, simultaneously targeting EGFR-TK to inhibit cell proliferation and Bcl-2 to restore apoptosis represents a promising strategy for the development of novel anticancer agents.

Various treatment strategies have been implemented to manage NSCLC, including chemotherapy, radiotherapy, surgery, immunotherapy, and molecularly targeted therapies [5]. Platinum based chemotherapy, such as cisplatin, remains a standard treatment option [6]. However, prolonged administration of cisplatin has been associated with various severe adverse effects including nausea, nephrotoxicity, Cardiotoxicity, hepatotoxicity and neurotoxicity [7]. The high toxicity to normal cells and the emergence of resistance to chemotherapy have driven the search for new anticancer agents that are safer and more specific. One promising strategy involves the utilization of biologically active constituents obtained from medical plants. Indonesia, renowned for its rich biodiversity, offers substantial potential for the advancement of plant-based anticancer therapies.one plant with considerable potential is Benalu batu, locally know as polohi wasu (*Begonia medicinalis*), an endemic species from Central Sulawesi that can be found growing both in the wild and through cultivation. Traditionally, this plant has been used to treat various diseases, including tumors [8].

Several in vitro studies have reported that Benalu batu can inhibit the growth of cancer cells such as HeLa and T47D [9], as well as MDA-MB and HT-29 cells [10], and can induce apoptosis in MCF7 and HCT-116 cells [8]. In addition, extracts of this plant have been reported to demonstrate antioxidant activity [11], immunostimulatory effects [12], and reduce neutrophil concentration in a colorectal cancer mouse model [13]. Nevertheless, to date `no studies have reported the anticancer activity of Benalu batu against lung cancer, particularly in the NSCLC model. In addition, studies comparing the anticancer potential of Benalu batu derived from wild and cultivated plants are still limited.

Therefore, this study aimed to evaluate the anticancer activity of wild and cultivated Benalu batu against A549 lung cancer cells as a model of NSCLC. As well as normal vero cells as a control. Bioactive compounds were identified using GC-MS, followed by molecular docking analysis with the target proteins EGFR-TK and Bcl-2 to explore the potential molecular mechanisms underlying their anticancer activity. To the best of our knowledge, this study is the first to evaluate the anticancer potential of both wild and cultivated Benalu batu against A549 lung cancer cells and to investigate its possible molecular mechanism through docking interactions with EGFR-TK and Bcl-2.

Materials and Methods

Sample collection

Figure 1 shows the Benalu batu samples used in this study. which were collected from two different locations in Nort Morowali Regency, Central Sulawesi, Indonesia. The wild Benalu batu samples were collected from the forest area in Wawopada Village (Figure 1a), whereas the cultivated Benalu batu were obtained from Toddopuli Ue Bangke Village (Figure 1b).

Figure 1. Habitus of Benalu batu. (a) Wild Benalu batu. (b) Cultivated Benalu batu.

Extraction of Benalu batu

The parts of wild and cultivated Benalu batu used in this study included both stems and leaves without separation. Prior to use, the plant material was cleaned and dried without direct exposure to sunlight. Once dried, the sample was ground into a simplicial powder. Each 120 grams of Benalu batu simplicial

powder was macerated with absolute ethanol (1:10) for 3 x 24 hours. The macerated solution underwent solvent removal through rotary evaporation maintained at 30°C under vacuum conditions, followed by further evaporation in an oven 35°C to ensure complete solvent removal, yielding a thick extract with a paste-like texture.

Cell culture

Cell cultivation was performed in the Parasitology Laboratory, Faculty of Medicine, Public Health, and Nursing, Universitas Gadjah Mada, following the CCRC Faculty of Pharmacy guidelines. A549 and Vero cells were grown in DMEM with 10% fetal bovine serum (FBS) and 1% penicillin-streptomycin, incubated at 37°C with 5% CO_2. At 80% confluency, cells were transferred to 96-well microtiter plates (5 x 10^4) and incubated for 24 hours for attachment.

Cytotoxicity test of extracts

Cytotoxicity assays were conducted following the protocol of CCRC UGM. A549 and Vero cells, which had been seeded in 96-well microtiter plates for 24 hours, were treated with extracts of wild and cultivated Benalu batu for 24 hours. The extract was first dissolved in dimethyl sulfoxide (DMSO) to prepare the stock solution and subsequently diluted with culture medium to obtain the desired concentration of 250 µg/mL, 125 µg/mL, 62.5 µg/mL, 31.25 µg/mL, 15.625 µg/mL, and 7.8125 µg/mL. The final concentration of DMSO in the wells is 0.5%. Each concentration was tested in three wells (technical triplicates). Two types of controls were included in the assay: a cell control (cells cultured in complete medium without tratment) and a media control (culture medium without cells). The evaluation of cytotoxic effects was conducted through the MTT assay. Each well received 100 µL of the MTT reagent and was incubated in a CO_2 environment for 4 hours to allow the formation of purple formazan crystals. After incubation, the absorbance of the contents in each well was determined using an ELISA microplate reader set to 595 nm.

Extract fractionation

Fractionation was carried out on the most potent extract. The fractionation process employed Vacuum Liquid Chromatography (VLC), using silica gel 60 F245 powder as the stationary phase. Elution was initiated with a non-polar solvent, n-hexane (10), followed sequentially by n-hexane (6): ethyl acetate (4), n-hexane (2): ethyl acetate (8), ethyl acetate (10), ethyl acetate (8): ethanol (2), ethyl acetate (6): ethanol (4), ethyl acetate (4): ethanol (6), ethyl acetate (2): ethanol (8), and finally the most polar solvent, ethanol (10), each eluent was used in a volume of 100 mL. The resulting fractions were collected in Erlenmeyer flasks and subsequently evaporated at room temperature.

Thin Layer Chromatography (TLC) profile and fraction pooling

The compound profiling was monitored across nine fractions using silica gel 60 F254 TLC plates. The mobile phase consisted of n-hexane and ethyl acetate with ratios of 4:1 [9] and 3:2. Spot visualization was carried out under visible light, as well as UV light at 254 and 366 nm. Similarities in spot patterns were used as a reference for the combination of fractions.

Combined fraction cytotoxicity test

The cytotoxicity assay procedures for the combined fractions on A549 and Vero cells followed the same steps as the cytotoxicity assay of Benalu batu extract. However, the concentration series used differed. For A549 cells, the concentration series for each fraction was 2.34 µg/mL, 4.69 µg/mL, 9.38 µg/mL, 18.75 µg/mL, 37.5 µg/mL, and 75 µg/mL, with the final DMSO concentration being 0.15%. For Vero cells, the concentration series was 75 µg/mL, 150 µg/mL, 300 µg/mL, 600 µg/mL, 1200 µg/mL, and 2400 µg/mL.

Analysis of bioactive compounds fractions

Characterization of bioactive constituents from the most promising fraction was performed at the Laboratorium Penelitian dan Pengujian Terpadu (LPPT), Universitas Gadjah Mada, utilizing Gas Chromatography-Mass Spectrometry (GC-MS) with a screening approach to identify potential bioactive compounds. The extract was solubilized in ethanol and homogenized through vortex mixing at 9500 rpm. Chromatographic separation was achieved using an HP-5MS UI column, with ultra-high purity (UHP) helium as the mobile phase at flow rate of 1 mL/min. The column temperature was initially maintained at 50^0C for 5 minutes, then ramped to 280^0C at a rate of 10^0C/min and held for 15 minutes. Compound detection was carried out with a transfer line temperature of 230^0C and mass scan range 40-500 m/z. The identification of chemical constituents was accomplished by comparing the retention times and mass spectral patterns with those available in standard reference libraries.

Lipinski's Rule of Five analysis of selected bioactive compounds

The Lipinski's Rule of Five analysis of selected bioactive compounds analysis was conducted in silico using the SwissADME web server (http://www.swissadme.ch/index.php) by retrieving the SMILES of each compound from PubChem and inputting them into SwissADME workspace. The evaluation of drug-like properties was conducted using the criteria outlined in Lipinski's Rule of Five.

Molecular docking

Molecular docking was executed utilizing the PyRx platform. The three-dimensional structure of the target proteins, EGFR-TK (PDB ID: 2ITY) and Bcl-2 (PDB ID: 4MAN), were retrieved from the Protein Data Bank (https://www.rcsb.org/). Protein preparation involved the elimination of crystallographic water molecules and native ligands using Discovery Studio. Ligand structures in SDF format were sourced from PubChem (https://pubchem.ncbi.nlm.nih.gov/) and performing energy minimization using Open Babel. Visualization of the molecular docking result was conducted using Discovery Studio.

Data analysis

Data analysis was performed using Microsoft Excel by first calculating the percentage of cell viability using the formula:

$$\%\ \text{viable cells} = \frac{\text{absorbance of treatment} - \text{absorbance of media control}}{absorbance\ of\ cell\ control - media\ control} x\ 100$$

The IC_{50} value was then determined through linear regression based on the regression equation y = ax+ b, data visualization was carried out using Origin 2025 software. The Selective Index (SI) is determined by calculating the ratio between the IC_{50} value of the compound in normal cells with its IC_{50} cancerous cells [14].

Results and Discussion

Cytotoxicity of wild and cultivated Benalu batu extracts against A549 and Vero cells

Figure 2 presents the results of cell viability measurements of A549 and Vero cells following treatment with ethanolic extracts of both wild and cultivated Benalu batu, across a concentration range of 7.8125-250 µg/mL. Cell viability analysis is essential for evaluating the anticancer potential of samples [15]. In this research, the MTT assay was employed to assess cell viability and the cytotoxicity levels of Benalu batu extracts. The MTT assay method utilizes a colorimetric approach evaluate cellular metabolic function, serving as an indirect indicator of the population of living cells [6]. As depicted in figure 2a, treatment administration led to a notable suppression of A549 cell viability. The wild-type Benalu batu extract demonstrated a superior cytotoxic response, exhibiting a more substantial decline in cell viability compared to its cultivated counterpart. Meanwhile, treatment of Vero cells with both types of extracts led to lower reduction in cell viability.

Figure 2b shows the cell viability after cisplatin treatment. In this study, cisplatin was employed as a positive control, given its established role as a standard chemotherapeutic agent in the management of NSCLC [16]. The viability of both A549 and Vero cells decreased more significantly after cisplatin treatment compared to treatment with either of the Benalu batu extracts, despite the narrower concentration range of cisplatin (6.25–200 µg/mL). In addition to cell viability, IC_{50} values also need to be analyzed to determine the concentration required to inhibit 50% of the target cells [17].

Based on the IC_{50} values presented Table 1, the wild and cultivated Benalu batu extracts exhibited IC_{50} values of 134.72 µg/mL and 178.63 µg/mL, respectively. The IC_{50} value serves as a benchmark for evaluating the cytotoxic potential of a compounds, as outlined by the guidelines of the National Cancer Institute, values ranging from 21 to 200 µg/mL indicate moderate cytotoxic activity, whereas values >500 µg/mL are considered non-toxic [18]. The IC_{50} values of the wild Benalu batu extract against Vero cells was 517.24 µg/mL, while that of the cultivated extract was 1.413.90 µg/mL. These findings are notable, as both extracts were non-toxic to normal Vero cells.

The non-toxic effects of both wild and cultivated Benalu batu extracts on normal Vero cells suggest a favorable safety profile and highlight a potential advantage over conventional chemotherapeutic agents such as cisplatin, which are often associated with toxicity toward normal cells due to their limited selectivity. Selective cytotoxicity toward cancer cells while sparing normal cells is an important characteristic of potential anticancer agents, as it may reduce damage to normal tissues and minimize adverse side effects during treatment [19]. Therefore, these findings suggest that Benalu batu extracts have promising potential to be further developed as safer anticancer candidates

To further evaluate the selectivity of the extracts toward cancer cells compared to normal cells the selectivity index (SI) was calculated [20]. As shown in Table 1, SI value of the wild Benalu batu extract is 3,84, whereas the cultivated Benalu batu extract has an SI 8,02. According to [23], an SI value greater than 3 indicates that an extract is more selective toward target (cancer) cells than normal cells. Meanwhile, the SI value of cisplatin is lower than that of the wild Benalu batu extract. These findings suggest that both wild and cultivated Benalu batu extracts exhibit greater selectivity than cisplatin, as a higher SI value indicates better selectivity [21].

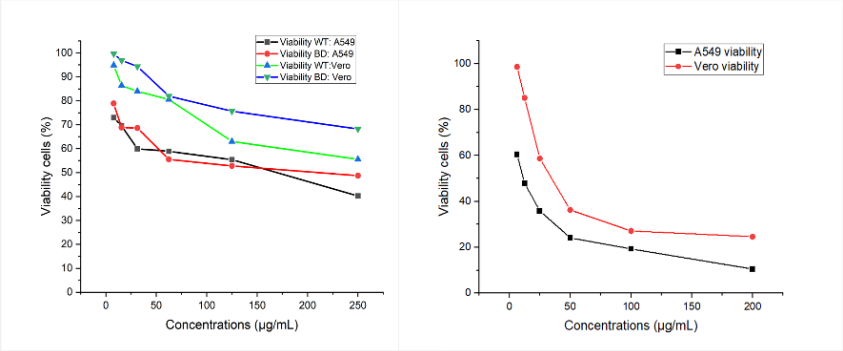

Figure 2. Viability of A549 and Vero cells after treatment. (a) Treatment with wild and cultivated Benalu batu extracts. (b) Treatment with cisplatin

The morphological changes of A549 cells following treatment with wild Benalu batu extract were also observed and are presented in Figure 3. In the control group, cells appeared to grow normally, forming a dense monolayer. However, after 24 hours of treatment with extract concentration ranging from 250 to 7.8125 µg/mL, the cells exhibited morphological alterations characterized by becoming small, round, shrunken, and detached. Treatment with the lowest concentration, 7.8125 µg/mL, did not result in significant morphological changes compared to the control cells. These findings suggest that cellular morphological changes are concentration-dependent.

Table 1. Cytotoxicity of Benalu batu extract and cisplatin on A549 and Vero cells.

	A549 cells			Vero cells			
	IC (µg/mL)	R^2	cytotoxic levels	IC (µg/mL)	R^2	cytotoxic levels	Selectivity Index (SI)
WT	134.71	0.91	Moderate	517.24	0.93	Non-toxic	3.84
BD	178.63	0.95	Moderate	1431.90	0.96	Non-toxic	8.02
CIS	10.81	0.98	Highly toxic	43.94	0.94	Moderate	4.07

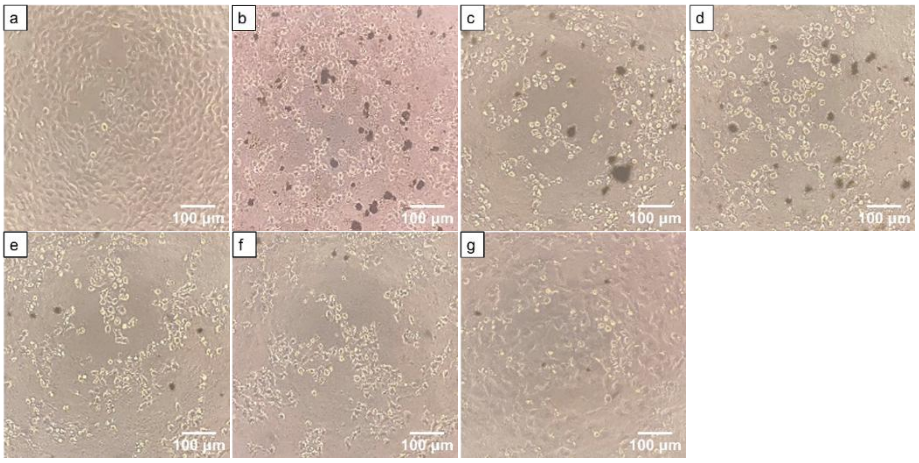

Figure 3. Morphology of A549 Cells After Treatment with Wild Benalu batu Extract. (A) control cells, (B) 250 µg/mL, (C) 125 µg/mL, (D) 62.5 µg/mL, (E) 31.25 µg/mL, (F) 15.625 µg/mL, (G) 7.825 µg/mL concentration.

Fractionation and Thin Layer Chromatography (TLC)

The extract displaying the most pronounced cytotoxic activity underwent systematic fractionation to isolate its constituent components, the wild Benalu batu extract. The purpose of fractionation is to separate the complex extract into simpler fractions based on their physical and chemical properties [22]. The fractionation process employed Vacuum Liquid Chromatography (VLC), a relatively simple method with adequate efficiency for compound separation based on polarity [23]. This experiment employed a series of nine eluent combinations forming a polarity gradient, spanning from non-polar to strongly polar solvents. The use of a polarity gradient eluent aims to maximize separation resolution and minimize cross-contamination between fractions [27]. The stationary phase used was silica gel 60 F254 powder. As a result of the fractionation process, nine fractions with varying polarities were obtained and further analyzed using Thin Layer Chromatography (TLC).

Figure 4 shows the separation of fractions obtained from the extract of wild Benalu batu. figure 4a shown the nine fractions eluted with n-hexane:ethyl acetate (4:1), exhibited a reasonably good separation, as indicated by the appearance of distinct spots in fractions 1, 2, and 3. This finding is consistent with the report by [24], which stated that n-hexane:ethyl acetate (4:1) is effective in separating compounds from Benalu batu extract. In the present study, fractions 1 and 2 showed clear spots that migrated far from the spotting line, suggesting that the compounds in these fractions are relatively non-polar, as non-polar compounds tend to elute more easily with non-polar [25]. Conversely, fraction 3 showed fewer spots, while fractions 4 through 9 did not display any visible spots. Therefore, the eluent polarity was increased to n-hexane:ethyl acetate (3:2) in an attempt to separate compounds in fractions 4-9. As shown in figure 4b, the higher polarity eluent successfully produced spots in fraction 4, however, no spots were observed in fractions 5 through 9.

The spots observed on the TLC plate were used as a reference for fraction combination. Similar spots indicate that corresponding fractions contain identical or similar compounds [26]. Fractions 1 and 2 exhibited similar spots and were therefore combined into fraction A. Likewise, fractions 3 and 4 showed comparable spots and were merged into fraction B. Meanwhile, fractions 5 through 9 did not display any spots and were consequently combined into fraction C.

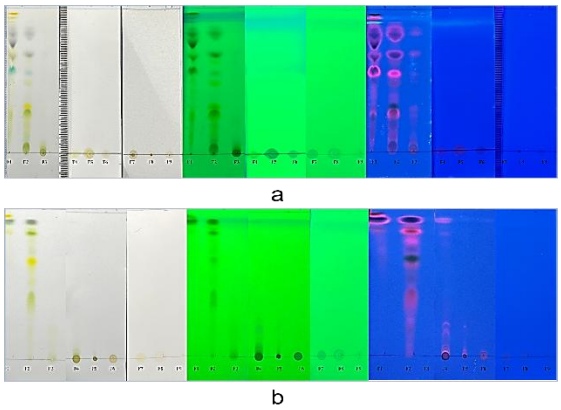

Figure 4. Thin Layer Chromatography of nine fractions of Benalu batu extract. (A) Eluent: n-hexane:ethyl acetate (4:1), (B) Eluent: n-hexane:ethyl acetate (3:2)

Cytotoxicity of the fractions against A549 and Vero cells

The viability of A549 cells and Vero cells after treatment with the wild Benalu batu fraction can be seen in Figure 5. Cytotoxicity assays of fractions A, B, and C were performed on A549 cells using a concentration range of 2.34375–75 µg/mL. Figure 5a shows that fraction A induced a significantly greater reduction in cell viability compared to fractions B and C. fraction A is a combined fraction obtained from the eluents of n-hexane (10) and n-hexane (6): ethyl acetate (4). These results indicate that fractions A is rich in non-polar to semi-polar compounds, which play a crucial role in the cytotoxicity effect on A549 cells. In figure 5b shows the viability of vero cells after treatment with the most toxic fraction, namly fraction A. this fraction was tested over a wider concentration range of 75-2400 µg/mL. the results indicate that fraction A gradually decreased Vero cell viability. To evaluated the cytotoxicity potency of the fractions against A549 and Vero cells, IC_{50} values were determined.

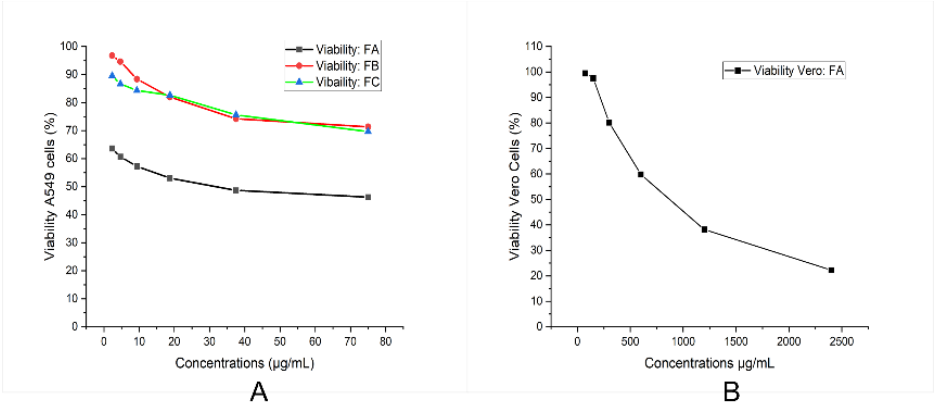

Figure 5. Cell viability after treatment with fractions of wild Benalu batu. (a) Viability of A549 cells, (b) Viability of Vero cells

Table 2 presents the IC_{50} values of fractions A, B, and C against A549 cells. Fraction A exhibited the strongest cytotoxic activity with an IC_{50} value of 33.93 µg/mL, whereas fractions B and C showed non-toxic activity, with IC_{50} values of 987.60 µg/mL and 3855.37 µg/mL, respectively. These results indicate that fraction A contains a higher concentration of compounds with potential anticancer activity. Interestingly, fraction A showed non-toxic activity against Vero cells (IC_{50} = 832 µg/mL) and exhibited a selectivity index (SI) of 24.52. This finding suggests that fraction A has high selectivity toward cancer cells. In general, an SI value ≥ 10 indicates high biological selectivity toward cancer cells [27]. A high SI value is an important parameter in anticancer drug development because it reflects the ability of a compound to selectively target cancer cells while minimizing toxic effects on normal cells during chemotherapy [28]. Moreover, a high SI value also indicates a wider therapeutic window, which is clinically significant because drug candidates with a broader therapeutic window are expected to produce lower toxic effects in cancer patients [29].

Table 2. Cytotoxicity of Wild Benalu batu Fractions and Cisplatin Against A549 and Vero Cells.

Sample	A549 cells			Vero cells			
	IC (µg/mL)	R^2	cytotoxic levels	IC (µg/mL)	R^2	cytotoxic levels	Selectivity Index (SI)
Cis	2.51	0.94	Highly toxic	43.94	0.94	Moderate	17.51
Faction A	33.93	0.99	Moderate	832	0.97	Non-toxic	24.52
Faction B	987.60	0.98	Non-toxic				
Faction C	3855.37	0.93	Non-toxic				

Figure 6 (b-g) illustrate the changes morphological of A549 cells observed under an inverted microscope following treatment with fraction A. In Figure 6a, untreated A549 cells exhibited typical epithelial morphology characterized by a cuboidal to polygonal shape, even distribution, and strong adherence to the culture surface. However, as shown in Figures 6b-g, treatment with fraction A resulted in noticeable morphological alterations. The cells appeared rounded, shrunken, dispersed, and detached from the surface. These morphological changes are indicative of cytotoxic effects and may suggest the induction of apoptotic or necrotic cell death. Furthermore, the reduced cell density and the presence of cellular debris indicate the high cytotoxicity activity of fraction A, which is consistent with the previously determined IC_{50} value. These result support the potential of fraction A as a promising anticancer agent against A549 cells.

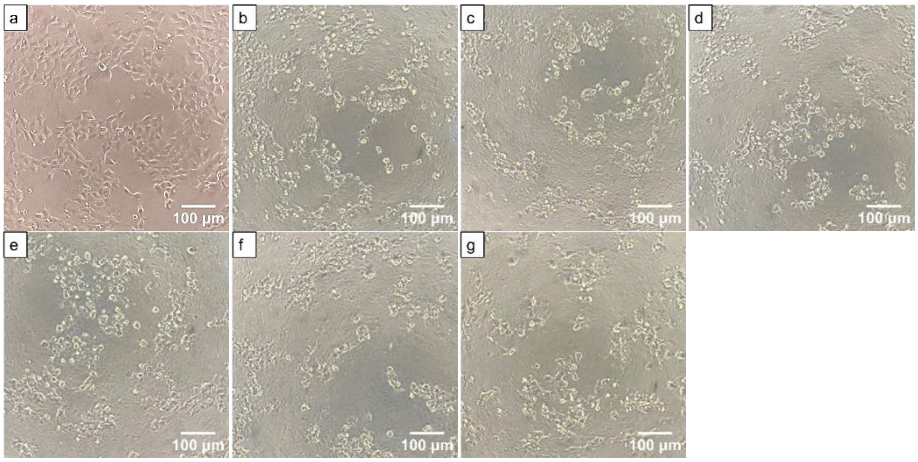

Figure 6. Morphology of A549 Cells after Treatment with Fraction A. (a) control cells, (b) 75 µg/mL concentration, (c) 37.5 µg/mL concentration, (d) 18.75 µg/mL concentration, (e) 9.38 µg/mL concentration, (f) 4.69 µg/mL concentration, (g) 2.34 µg/mL concentration

Based on the morphological observations of Vero cells after treatment with fraction A at various concentrations, dose-dependent morphological changes were observed (Figure 7a-g). In the control group (Figure 7a), Vero cells exhibited a normal elongated epithelial shape, with intact cell membranes and uniform distribution. However, at higher concentrations, specifically 2.400 µg/mL (figure 7b) and 1.200 µg/mL (Figure 7c), significant morphological damage was still evident but less severe compared to the higher concentrations. As the concentration decreased, such as at 300 µg/mL (Figure 7e) and 150 µg/mL (Figure 7f), cell morphology began to recover and approached normal conditions. Finally, at 75 µg/mL (figure 7g), cells exhibited minimal morphological alterations, resembling the control condition. These findings suggest that fraction A exerts cytotoxic effects on Vero cells at high concentrations but is relatively safe at lower concentrations.

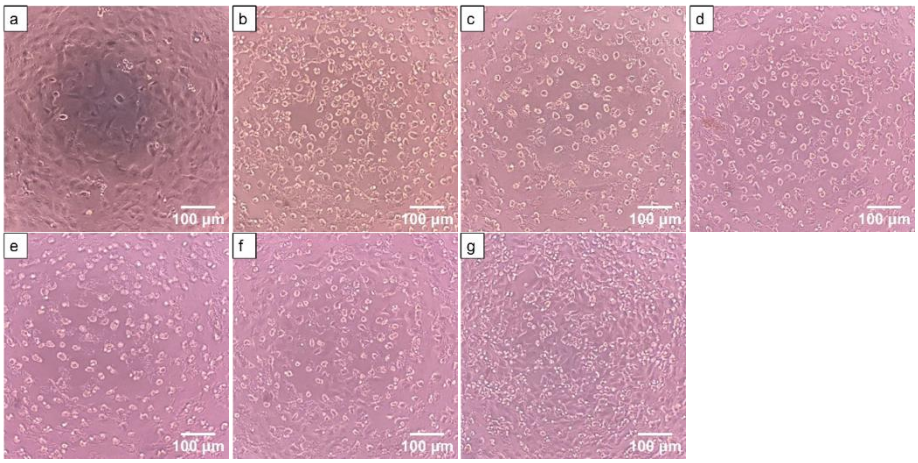

Figure 7. Morphology of Vero cells after treatment with Fraction A. (a) cell control, (b) 2400 µg/mL concentration, (c) 1200 µg/mL concentration, (d) 600 µg/mL concentration, (e) 300 µg/mL concentration, (f) 150 µg/mL concentration, (g) 75 µg/mL concentration.

Bioactive compounds in fraction A

Based on GC-MS analysis, fraction A of the wild Benalu batu extract contains a total 52 compounds (Figure 8), eight of which show potential anticancer activity. This is indicated by the highest peak area values of these compounds, which reflect their relative concentrations in the sample the greater the peak area value, the higher the concentration [34]. Tabble 3 the identification results show that the compound with the highest peak area is stigmasterol (19.80%), followed by campesterol (7.06%), neophytadiene (4.83%), sitosterol (3.29%), squalene (2.73%), phytol (2.39%), phytol acetate (1.221%), ethyl iso-allocholate (1.70%), and α-tocopheryl acetate (1.10%). The composition based on peak area indicates a dominance of phytosterols from the steroid group in fraction A, suggesting the presence of diverse

compounds with varying characteristics, thereby reinforcing the chemical profile and potential bioactivity of the fraction.

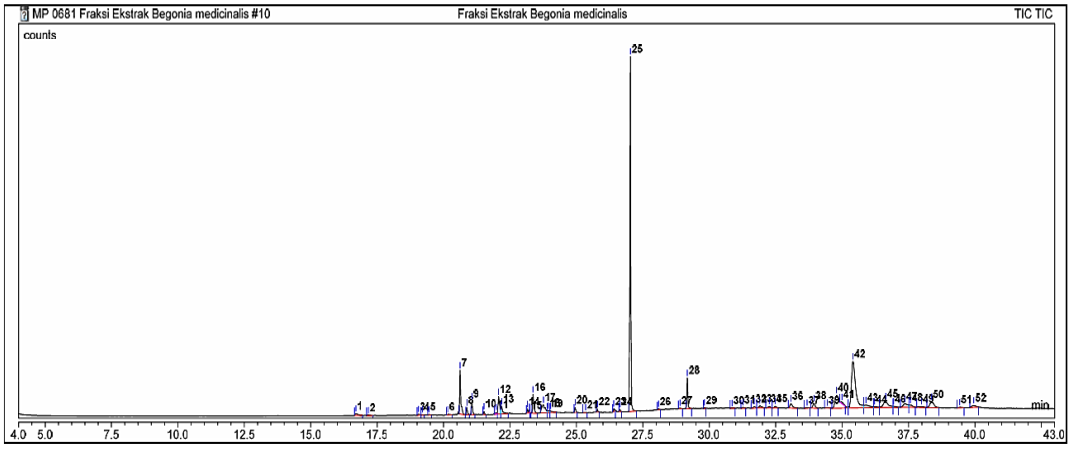

Figure 8. GC-MS chromatogram of bioactive compounds in fraction A of wild Benalu batu

Eight compounds with the highest peak area percentages exhibited certain characteristics. Several compounds identified through GC–MS analysis in this study have previously been reported to exhibit anticancer activities in various experimental models. In particular, phytosterols such as stigmasterol, campesterol, and sitosterol are known to possess biological activities including antiproliferative and pro-apoptotic effects against several cancer cell lines. Therefore, the presence of these compounds in fraction A of wild Benalu batu suggests a potential contribution to the observed anticancer activity.

Stigmasterol is a type of phytosterol classified as a steroid, featuring a tetracyclic (6-6-6-5) chemical structure and amphiphilic properties due to the presence of a hydroxyl group [35]. This compound is synthesized via the mevalonate pathway [36]. The anticancer activity of stigmasterol has been widely reported [37] showed that stigmasterol inhibits proliferation and metastasis and induces apoptosis in various cancer cells, including breast, lung, liver, and ovarian cancers. Campesterol is a phytosterol has a long side chain consisting of 28 carbon atoms (C28) and a hydroxyl group at the C-3 position [38], Campesterol has been reported to induce apoptosis in human ovarian [39], and liver cancer cells [40]. Neophytadiene is a diterpenoid formed through chlorophyll degradation via the mevalonate pathway [41]. This compound exhibits cytotoxic activity against A549 and PC-3 cancer cells [42]. Sitosterol is also a steroidal phytosterol synthesized through the mevalonate pathway [43], Sitosterol has the ability to induce apoptosis and cell cycle arrest in breast, prostate, and pancreatic cancers through the regulation of the PI3K/Akt, NF-κB, and caspase signaling pathways [44]. Squalene, a natural lipid compound from the triterpene hydrocarbon group [45], squalene has been reported to inhibit proliferation, induce apoptosis, and arrest the cell cycle in Caco-2 colon cancer cells [46]. Phytol is a long-chain unsaturated acyclic diterpene alcohol, synthesized from chlorophyll degradation during leaf senescence [47]. Phytol exhibits strong antiproliferative activity against A549 cells [48]. Phytol acetate is an ester derivative a terpene alcohol commonly [49], this compound also shows anticancer activity [50], and α-Tocopheryl acetate is a semi-polar ester form of vitamin E derivative (α-Tocopherol) [51]. In addition, α-tocopherol and especially its oxidation products exhibit cytotoxic effects against MCF-7 and PC-3 cells [52].

Table 3. GC-MS Analysis of Bioactive Compounds in Fraction A of Wild Benalu batu

No peak	Compounds name	Formula	Structure	Molecular weight	Rt	Peak areas (%)
7	Neophytadiene	C20H38	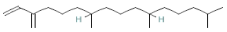	278	20.62	4.83
9	Phytol, acetate	C22H42O2	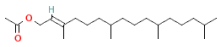	338	21.07	1.221
16	Phytol	C20H40O		296	23.37	2.39
28	Squalene	C30H50	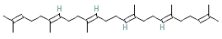	410	29.18	2.73
38	α-Tocopheryl acetate	C31H52O3	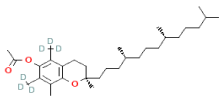	471	33.94	1.10
40	Campesterol	C28H48O	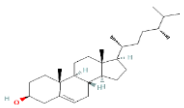	400	34.79	7.06
42	Stigmasterol	C29H48O	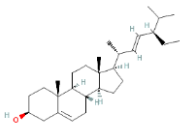	412	35.41	19.80
45	Sitosterol	C29H50O	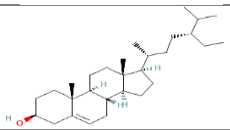	414	36.64	3.29

Lipinski's properties of selected bioactive compounds

Table 4 presents the results of the Lipinski's Rule of Five analysis for eight compounds predicted to have anticancer potential. The Rule of five proposed by Lipinski provides a framework for assessing the potential of chemical compounds to be developed as orally active drugs [53]. The guideline outlines four key criteria: a molecular mass not exceeding 500 Daltons, a maximum of five hydrogen bond donors, no more than ten hydrogen bond acceptors, and a partition coefficient (LogP) of five or lower. Ideally, a compound should violate no more than one of these criteria to be considered drug-like [54]. The analysis showed that all compounds met the thresholds for hydrogen bond donors (≤5) and acceptors (≤10). The presence of hydrogen bond donors and acceptor in a molecule plays a crucial role in its capacity to cross cellular membranes, an excessive number of these groups may impede membrane penetration and consequently lower the compounds bioavailability [55]. Phytol acetate, squalene, α-tocopheryl acetate, stigmasterol, and sitosterol exhibited LogP values greater than 5, indicating that these compounds are highly lipophilic [23]. LogP reflects the compound's solubility balance between aqueous and lipid environments, a value of ≤5 is considered ideal for optimal cell permeability, which is essential for oral drug potential [54]. These findings suggest that all eight analyzed compounds still meet the criteria of Lipinski's Rule of Five, despite some violating one of the parameters.

Table 4. Lipinski's Rule of Five of Selected Bioactive Compounds from Fraction A of Wild Benalu batu Analyzed Using SwissADME

Compounds	MW (≤500)	H-bounds acceptors (≤10)	H-bond donors (≤5)	iLogP (≤5)
Neophytadiene	278.52	0	0	5.0
Phytol, acetate	338.57	2	0	5.46
Phytol	296.53	1	1	4.85
Squalene	410.72	0	0	10.605
α-Tocopheryl acetate	472.74	3	0	6.28
Campesterol	400.68	1	1	4.97
Stigmasterol	412.69	1	1	5.08
Sitosterol	414.71	1	1	5.05

Molecular docking protein EGFR

The molecular docking study targeted the EGFR kinase domain protein (PDB ID: 2ITY), which is co-crystallized with Gefitinib (Iressa), a tyrosine kinase inhibitor commonly employed in treating NSCLC. This structure represents the wild-type form of EGFR-TK, providing critical insights into the binding interactions and inhibitory mechanism of Gefitinib on EGFR-TK activity. Docking of compounds from fraction A of wild Benalu batu to this structure aimed to identify potential mechanisms of EGFR-TK inhibition that are similar to or more effective than Gefitinib.

Table 5 presents the docking results of eight bioactive compounds from fraction A of wild Benalu batu. In docking studies, the binding affinity value serves as a key parameter for determining the strength and stability of ligand-protein interactions, thus allowing for the screening of potential drug candidates, a more negative binding affinity indicates a stronger interaction at the protein's active site [56]. Based on the docking analysis, three compounds had more favorable binding affinity values than Gefitinib, namely Campesterol, Stigmasterol, and Sitosterol. Beyond binding affinity, the Root-Mean-Square Deviation (RMSD) value serves as a critical parameter for evaluating the precision and reliability of docking outcomes by comparing the predicted ligand conformation to its experimentally determined crystallographic structure. An RMSD value below 2 Å indicates high accuracy [57]. The docking results of the eight compounds yielded an RMSD value of 0, indicating a high level of accuracy as it closely resembles the actual crystal structure.

Table 5. Molecular Docking Analysis of Bioactive Compounds from Fraction A of Wild Benalu batu Against EGFR-TK

Ligand	Binding Affinity	Rmsd ub/lb	Interaction
Gefitinib (kontrol)	-7.7	0	**Conventional Hydrogen Bond:** MET793 **Halogen:** LEU788 **Pi-Cation**: LYS745 **Pi-Anion**: ASP855 **Pi-Sigma**: LYS745 **Alkyl**: LEU718, VAL726, ALA743, LEU844, LYS745 **Pi-Alkyl**: VAL726
Neophytadiene	-5.6	0	**Alkyl**: ALA743, CYS797, LEU844, MET793, LEU844, LEU718, LEU792, VAL726, MET766, CYS775
Phytol, acetate	-5.3	0	**Alkyl:** ALA743, LEU718, LEU792, VAL726, LEU844
Phytol	-5.8	0	**Alkyl:** ALA743, CYS797, LEU844, VAL726, LYS745, LEU718, LEU792, MET793
Squalene	-6.4	0	**Alkyl:** ALA743, VAL726, LYS745, LEU844, CYS797, MET793
α-Tocopheryl acetate	-7.1	0	**Alkyl:** LEU718, ALA743, MET793, LEU844, EU718, VAL726, YS745, CYS797 **Pi-Alkyl:** LEU718
Campesterol	-9.2	0	**Alkyl:** LEU718, VAL726, ALA743, LEU844, MET766, CYS775, LYS745, LEU788
Stigmasterol	-9.1	0	**Alkyl**: LEU718, VAL726, ALA743, LEU844, CYS797, LYS745, MET766, LEU788
Sitosterol	-8.2	0	**Alkyl:** LEU718, VAL726, ALA743, LEU844, CYS797, LYS745, LEU788, MET766, CYS775

The 2D visualization of ligand protein interactions revealed key residue interactions at the binding site of the target protein. Based on the interaction analysis at the active site of the EGFR-TK protein, as shown in Figure 9, differences were observed in the types of interactions between the control ligand and the compounds from wild Benalu batu. Figure 9a illustrates that Gefitinib interacts with the target protein through multiple interactions, including a hydrogen bond with MET793 in the hinge region, halogen bonds with residue LEU788; Pi-Cation and Pi-Sigma interactions with LYS745; a Pi-Anion interaction with ASP855; and hydrophobic alkyl interactions with residues LEU718, VAL726, ALA743, LEU844, and LYS745. In contrast, the compounds from wild Benalu batu exhibited only hydrophobic interactions, specifically alkyl and Pi-alkyl interactions.

Figure 9b illustrates the visualization of Campesterol binding to the EGFR-TK protein. Campesterol showed a strong binding affinity toward EGFR-TK (−9.2 kcal/mol), which involved interactions with several amino acid residues. Total of 14 alkyl interactions were observed with residues LEU718, VAL726, ALA743, LEU844, MET766, CYS775, LYS745, and LEU788. Compared to Gefitinib, there are notable differences in the interacting residues. Specifically, Gefitinib does not exhibit interactions with MET766 and CYS775. MET766 serves as a critical component of the Regulatory spine (R-spine) within EGFR-TK, acting as a structural element vital for enzymatic function and positioned at the C-terminal region of the αC-helix [58]. These findings differ from those of [59] who reported that Gefitinib interacts with MET766, which h contributes to stabilizing the phenyl ring of Gefitinib. Moreover, the interaction of campesterol with CYS775 is particularly noteworthy, as this non-conserved residue is situated in a chemically restricted and relatively non-polar region at the back of the ATP-binding pocket [60] and plays an important role in stabilizing ligand binding [59].

The interaction of stigmasterol with the active site of EGFR-TK is shown in Figure 9c. Interactions were observed with key residues, including LEU718, VAL726, ALA743, LEU844, CYS797, LYS745, MET766, and LEU788. However, several interaction differences were noted compared to those formed by Gefitinib, particularly with residues CYS797, MET766, and LEU788. CYS797 refers to a cysteine residue situated in the active site of the EGFR tyrosine kinase domain, specifically positioned at the N-terminal portion of the α-helix adjacent to the ATP-binding hinge region [61]. Additionally, in the Gefitinib complex, the interaction with LEU788 occurs via a halogen bond, whereas in the stigmasterol complex, it occurs through a hydrophobic interaction.

The residue interactions formed by the sitosterol compound are presented in Figure 9d. The interacting residues are similar to those observed with stigmasterol, including LEU718, VAL726, ALA743, LEU844, CYS797, LYS745, LEU788, MET766, and CYS775. The distinct interactions compared to Gefitinib involve LEU788, CYS797, and MET766. The interaction with residue LEU844 plays a crucial role in stabilizing ligand-protein binding, as also observed with known inhibitors such as Lafatinib and Erlotinib [59]. All the evaluated compounds established interactions with critical amino acid residues situated within the highly conserved and hydrophobic ATP-binding site of EGFR-TK, specifically within the N-lobe at the N-terminal region, which is relatively small and dominated by β-sheet structures and the α-C helix [62].

To better interpret the docking performance of the identified compounds, their binding affinities were compared with several phytochemicals previously reported as EGFR inhibitors. Previous studies have reported comparable binding energies for certain phytochemicals. For example, [63] reported that Withastramonolide displayed the same binding energy as campesterol (−9.2 kcal/mol) against EGFR-TK, with interactions primarily dominated by hydrophobic contacts. Additionally, kaempferol was reported to have a higher binding energy than sitosterol (−8.3 kcal/mol), likely due to the presence of hydrogen bond interactions, as observed in prior research. Conversely, some phytochemicals exhibited lower binding affinities compared to the top three compounds in this study. For instance, curcumin (−8.0 kcal/mol) and zerumbone (−7.6 kcal/mol) [64], as well as ellagic acid (−8.8 kcal/mol), myricetin (−8.9 kcal/mol), and phlorizin (−8.7 kcal/mol) [65], showed comparatively weaker interactions. These comparisons suggest that campesterol, stigmasterol, and sitosterol exhibit relatively strong binding affinities toward EGFR-TK compared with several previously reported phytochemicals.

a

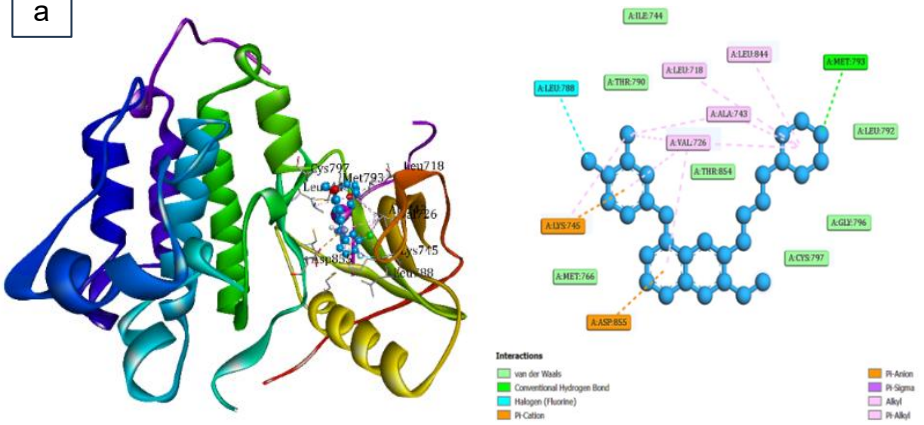
A:ILE:744
A:LEU:844
A:MET:793
A:LEU:718
A:THR:790
A:LEU:788
A:ALA:743
A:LEU:792
A:VAL:726
A:THR:854
A:LYS:745
A:GLY:796
A:CYS:797
A:MET:766
A:ASP:855
Interactions
van der Waals
Conventional Hydrogen Bond
Halogen (Fluorine)
Pi-Cation
Pi-Anion
Pi-Sigma
Alkyl
Pi-Alkyl

b

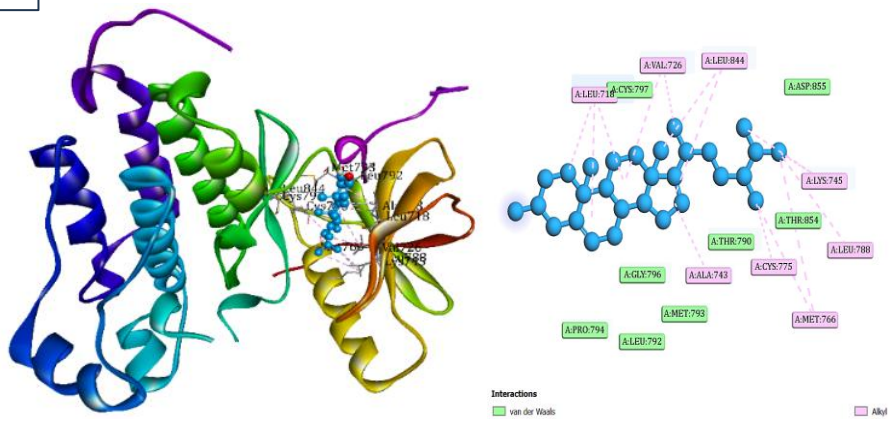
A:VAL:726
A:LEU:844
A:LEU:718
A:CYS:797
A:ASP:855
A:LYS:745
A:THR:854
A:THR:790
A:LEU:788
A:CYS:775
A:GLY:796
A:ALA:743
A:MET:793
A:MET:766
A:PRO:794
A:LEU:792
Interactions
van der Waals
Alkyl

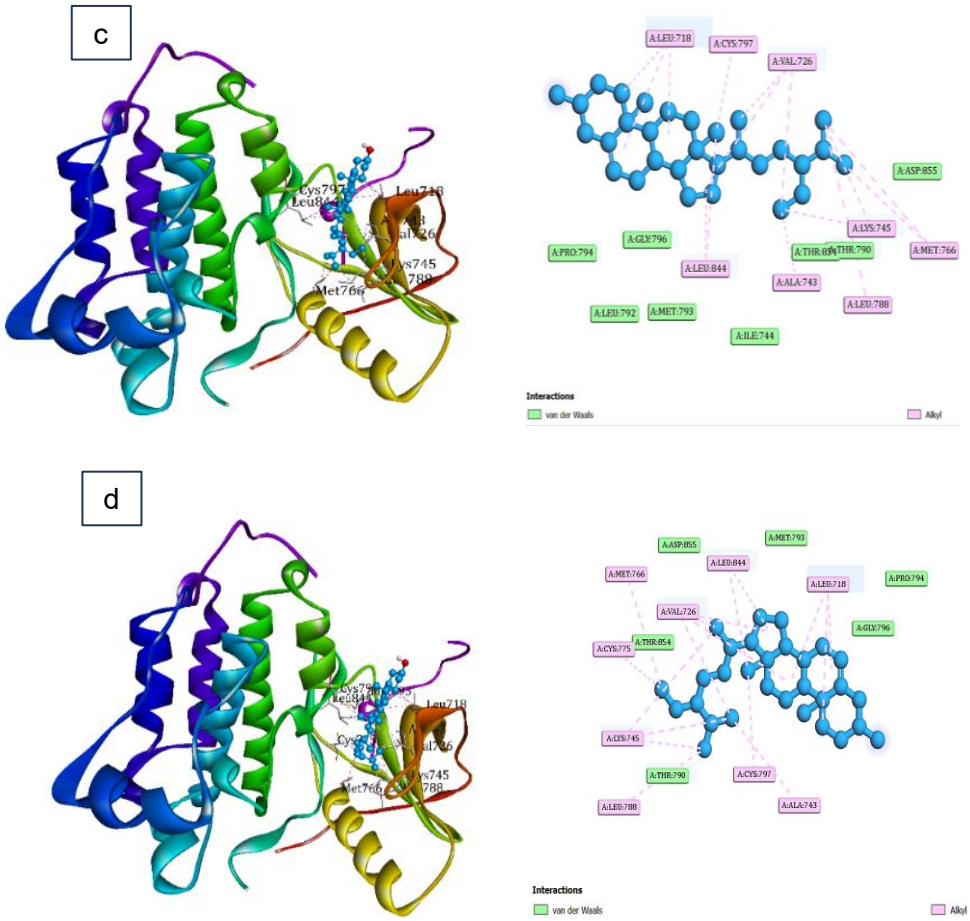

Figure 9. Visualization of the interaction between Benalu batu compounds and EGFR-TK protein. (A) Gefitinib, (B) Campesterol, (C) Stigmasterol, (D) Sitosterol.

Molecular docking protein Bcl-2

The compounds isolated from the wild Benalu batu fraction were further examined through molecular docking against B-cell lymphoma 2 (Bcl-2) protein, which functions as an inhibitor of apoptosis. This protein is characterized by the presence of BH1, BH2, BH3, and BH4 domains. Pro-apoptotic proteins such as BID, BIM, PUMA, NOXA, and BAD, which possess the BH3 domain, can bind to the hydrophobic pocket of Bcl-2, thereby disrupting its function in inhibiting apoptosis [66]. Therefore, molecular docking of wild Benalu batu compounds was performed to identify specific interactions at the BH3 domain active site. In this study, the 3D structure of the wild type Bcl-2 (PDB ID: 4MAN) was used. This structure has a high resolution of 2.07 Å, making it suitable for docking modeling.

Table 6 presents the results of the docking analysis of bioactive compounds from fraction A of wild Benalu batu against Bcl-2. The compounds with the strongest binding affinity were Sitosterol (-8.7 kcal/mol), followed by Squalene (-8.5 kcal/mol), Stigmasterol (-8.5 kcal/mol), and Campesterol (-8.4 kcal/mol). In contrast, the four compounds with the weakest binding affinities were Neophytadiene (6.0 kcal/mol), Phytol (-6.0 kcal/mol), Phytol acetate (-6.9 kcal/mol), and α-Tocopheryl acetate (-7.9 kcal/mol). The RMSD analysis showed that all compounds had an RMSD value of 0, indicating a high degree of fit with the model used.

Table 6. Molecular Docking Analysis of Bioactive Compounds from Fraction A of Wild Benalu batu Against Bcl-2

Ligand	Binding Affinity	RMSD ub/lb	Interaction
Neophytadiene	-6.0	0	**Alkyl**: ALA146, ARG143, LEU134, MET112, VAL130, VAL153 **Pi-Alkyl:** PHE101, PHE109
Phytol, acetate	-6.9	0	**Alkyl:** ALA146, ARG143, MET112, VAL153 **Pi-Alkyl:** PHE101, PHE109, TYR105
Phytol	-6.0	0	**Carbon Hydrogen Bond:** GLY142 **Alkyl:** VAL130, LEU134, MET112, VAL153 **Pi-Alkyl:** PHE101, TYR105, PHE109
Squalene	-8.5	0	**Pi-Sigma**: TYR105, TYR199 **Alkyl:** ALA146, LEU134, MET112, VAL153, VAL145 **Pi-Alkyl:** PHE101, PHE109, PHE195, TYR199
α-Tocopheryl acetate	-7.9	0	**Pi-Sigma:** TYR199 **Alkyl:** ALA146, LEU134, VAL130, ARG143, VAL145 **Pi-Alkyl:** PHE101, TYR105, TYR199, LEU134
Campesterol	-8.4	0	**Alkyl:** LEU134, ARG143, ALA146, MET112 **Pi-Alkyl:** PHE101, PHE105
Stigmasterol	-8.5	0	**Alkyl**: LEU134, ARG143, ALA146, MET112, LEU134 **Pi-Alkyl:** PHE101, TYR105, PHE109, PHE150
Sitosterol	-8.7	0	**Alkyl:** LEU134, ARG143, ALA146, MET112, VAL153 **Pi-Alkyl:** PHE101, TYR105, PHE109, PHE150

Figure 10 a-c shows the docking visualization was performed on compounds with the strongest binding affinity values, namely Squalene, Campesterol, Stigmasterol, and sitosterol. The squalene compound (Figure 10a) formed Pi-sigma interactions with TYR105 and TYR199, along with alkyl interactions with ALA146, LEU134, MET112, VAL153, and VAL145. Meanwhile, the campesterol compound (Figure 10b) exhibited alkyl bonds with LEU134, ARG143, ALA146, and MET112, as well as Pi-alkyl interactions with PHE101 and PHE105. The stigmasterol compound (Figure 10c) showed a similar interaction pattern, involving alkyl bonds with LEU134, ARG143, ALA146, and MET112, and Pi-alkyl interactions with PHE101, TYR105, PHE109, and PHE150. Figure 10 d the 2D visualization of sitosterol revealed hydrophobic alkyl interactions with residues ARG143, ALA146, MET112, VAL153, and LEU134, as well as Pi-alkyl interactions with residues PHE101, TYR105, PHE109, and PHE150. Squalene, campesterol, stigmasterol, and sitosterol interacted with the Bcl-2 protein predominantly through hydrophobic alkyl and Pi-alkyl interactions involving nonpolar and aromatic amino acid residues.

In general, the binding between the ligands and the Bcl-2 protein is mainly governed by hydrophobic forces, involving similar amino acid residues. These interactions occur because the compounds derived from Benalu batu tend to be lipophilic (hydrophobic), which facilitates binding to key residues within the conserved hydrophobic groove of Bcl-2 [68]. The compounds with the strongest binding affinities all exhibit interactions with residues ARG143, PHE10, TYR105, PHE109, TYR199, MET112, VAL153, and LEU134 residues that are also known to interact with Navitoclax, know Bcl-2 inhibitor [68]. Therefore, these findings suggest that most of the residue interactions occur within the BH3 domain of the Bcl-2 protein.

Several compounds have also been reported in molecular docking studies targeting the Bcl-2 protein. A study by [69] reported that myricetin exhibited relatively weak binding affinity toward Bcl-2, with a value of −7.3 kcal/mol, involving hydrophobic interactions with residues PHE63 and GLY104 as well as hydrogen bonds with ARG66, PHE63, and TYR67. In addition, galangin showed the same binding affinity value (−7.3 kcal/mol) with hydrophobic interactions at residue PHE63, while apigenin and fisetin demonstrated binding affinities of −7.2 kcal/mol and −7.1 kcal/mol, respectively. These findings indicate that hydrophobic interactions may play an important role in enhancing the stability and strength of ligand interactions with the Bcl-2 protein. Furthermore, a study by [70] reported several other compounds, including D-limonene, caffeic acid, isocinnamic acid, and friedelin, with binding affinity values of −5.5, −6.6, −5.9, and −10.1 kcal/mol, respectively. Among these compounds, friedelin exhibited the strongest binding affinity, mediated by interactions with residues VAL, TYR, and ALA, which are also frequently observed in the residue interactions identified in this study. This comparison suggests that squalene, stigmasterol, campesterol, and sitosterol may serve as promising anticancer candidates worthy of further investigation. However, since the present study is still limited to in vitro and in silico approaches, further studies through in vivo experiments are required to evaluate the anticancer potential of Benalu batu and to confirm its interaction mechanisms with the EGFR-TK and Bcl-2 proteins in biological systems

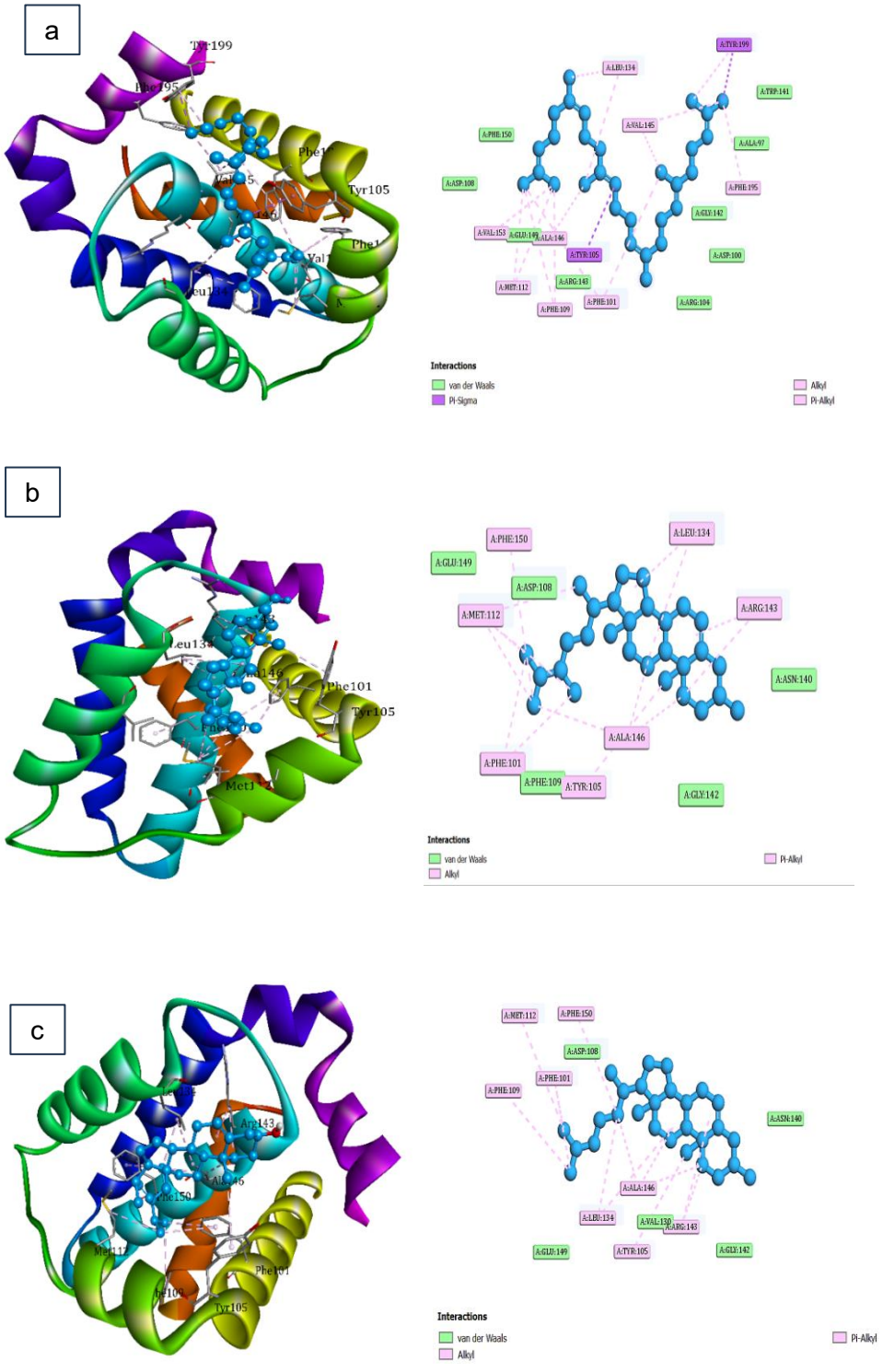
a
Tyr105
Interactions
van der Waals
Pi-Sigma
Alkyl
Pi-Alkyl
b
Phe101
Tyr105
Met1
A:PHE:150
A:LEU:134
A:GLU:149
A:ASP:108
A:MET:112
A:ARG:143
A:ASN:140
A:ALA:146
A:PHE:101
A:PHE:109
A:TYR:105
A:GLY:142
Interactions
van der Waals
Alkyl
Pi-Alkyl
c
Arg143
Phe150
Met112
Phe101
Phe109
Tyr105
A:MET:112
A:PHE:150
A:ASP:108
A:PHE:101
A:PHE:109
A:ASN:140
A:ALA:146
A:LEU:134
A:VAL:130
A:ARG:143
A:GLU:149
A:TYR:105
A:GLY:142
Interactions
van der Waals
Alkyl
Pi-Alkyl

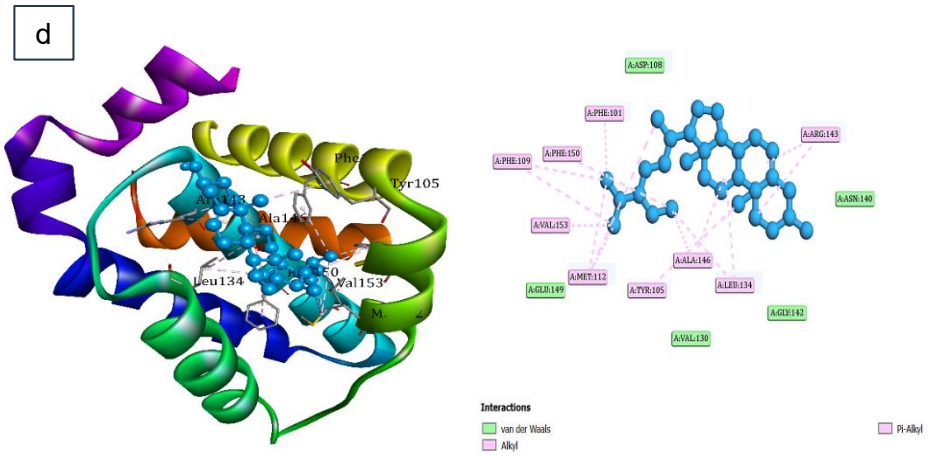

Figure 10. Visualization of the interaction between Benalu batu compounds and the Bcl-2 protein. (A) Squalene, (B) Campesterol, (C) Stigmasterol, and (D) sitosterol.

Conclusions

In conclusion, the ethanolic extract of wild Benalu batu exhibited higher cytotoxic activity compared to the extract from cultivated plants, with an IC_{50} value of 134.71 µg/mL and was non-toxic to Vero cells (IC_{50} of 517.24 µg/mL). Chromatographic profile analysis revealed that the compounds in the wild Benalu batu extract were predominantly non-polar. Cytotoxicity testing of potential fractions from the wild Benalu batu extract identified Fraction A as the most potent, with an IC_{50} of 33.93 µg/mL and a high selectivity index of 24.52 against cancer cells. GC-MS analysis identified eight bioactive compounds presumed to have anticancer activity. Molecular docking studies against the EGFR-TK protein showed that campesterol (-9.2 kcal/mol), stigmasterol (-9.1 kcal/mol), and sitosterol (-8.2 kcal/mol) had more favorable binding affinity values than the control (gefitinib, -7.7 kcal/mol). Against the Bcl-2 protein, sitosterol exhibited the highest binding affinity (-8.7 kcal/mol), followed by squalene and stigmasterol (-8.5 kcal/mol), and campesterol (-8.4 kcal/mol). Based on the results of this study, wild Benalu batu has the potential to be further investigated and developed as a candidate for anticancer therapy in the treatment of non-small cell lung cancer (NSCLC). This study is the first to evaluate the anticancer potential of wild and cultivated Benalu batu against NSCLC (A549 cells) and to explore its possible molecular mechanisms through interactions with EGFR-TK and Bcl-2 proteins using *in silico* analysis. However, as this research represents a preliminary study, further investigations including more comprehensive *in vitro* studies and subsequent *in vivo* experiments are required to confirm its potential as a candidate for anticancer therapy.

Conflicts of interest

The author declares that there is no conflict of interest regarding the publication of this paper.

Acknowledgment

The author expresses sincere gratitude to the Lembaga Pengelola Dana Pendidikan (LPDP) for the financial support provided for this thesis research.

References

[1] Provencio, M., Nadal, E., Gonzalez-Larriba, J. L., Martinez-Marti, A., Bernabé, R., Bosch-Barrera, J., ... & Romero, A. (2023). Perioperative nivolumab and chemotherapy in stage III non–small-cell lung cancer. *New England Journal of Medicine*, *389*(6), 504-513. https://doi.org/10.1056/NEJMoa2215530

[2] Ciardiello, F., Hirsch, F. R., Pirker, R., Felip, E., Valencia, C., & Smit, E. F. (2024). The role of anti-EGFR therapies in EGFR-TKI-resistant advanced non-small cell lung cancer. *Cancer Treatment Reviews*, *122*, 102664. https://doi.org/10.1016/j.ctrv.2023.102664

[3] Prabhakar, C. N. (2015). Epidermal growth factor receptor in non-small cell lung cancer. *Translational lung cancer research*, *4*(2), 110. https://doi.org/10.3978/j.issn.2218-6751.2014.09.15

[4] Qian, S., Wei, Z., Yang, W., Huang, J., Yang, Y., & Wang, J. (2022). The role of BCL-2 family proteins in regulating apoptosis and cancer therapy. *Frontiers in oncology*, *12*, 985363. https://doi.org/10.3389/fonc.2022.985363

[5] Alduais, Y., Zhang, H., Fan, F., Chen, J., & Chen, B. (2023). Non-small cell lung cancer (NSCLC): A review of risk factors, diagnosis, and treatment. *Medicine*, *102*(8), e32899. https://doi.org/10.1097/MD.0000000000032899

[6] Bahuguna, A., Khan, I., Bajpai, V. K., & Kang, S. C. (2017). MTT assay to evaluate the cytotoxic potential of a drug. *Bangladesh Journal of Pharmacology*, *12*(2), 115–118. https://doi.org/10.3329/bjp.v12i2.28686

[7] Aldossary, S. A. (2019). Review on pharmacology of cisplatin: clinical use, toxicity and mechanism of resistance of cisplatin. *Biomedical and Pharmacology Journal*, *12*(1), 7-15 https://doi.org/10.13005/bpj/1608

[8] Zubair, M. S., Alarif, W. M., Ghandourah, M. A., Anam, S., & Jantan, I. (2020). Cytotoxic activity of 2-o-β-glucopyranosil cucurbitacin d from benalu batu (Begonia sp.) growing in Morowali, Central Sulawesi. *Indonesian Journal of Chemistry*, *20*(4), 766–772 https://doi.org/10.22146/ijc.48421

[9] Anam, S., Ritna, A., Dwimurti, F., Rismayanti, D., & Sulaiman Zubair, M. (2014). Aktivitas Sitotoksik Ekstrak Metanol Benalu Batu (Begonia sp.): Ethnomedicine Suku Wana Sulawesi Tengah (Cytotoxic Activity of Benalu Batu (Begonia sp.) Methanolic Extract: An Ethnomedicine of Wana Tribe Central Sulawesi). *Jurnal Ilmu Kefarmasian Indonesia*, *9*(1), 10–16 https://doi.org/10.33376/ikfi.v9i1.10

[10] Prihardina, B., & Fatmawati, S. (2021, November). Cytotoxicity of Begonia medicinalis aqueous extract in three cancer cell line. In *IOP Conference Series: Earth and Environmental Science* (Vol. 913, No. 1, p. 012084). IOP Publishing. https://doi.org/10.1088/1755-1315/913/1/012084

[11] Zubair, M. S., Khairunisa, S. Q., Sulastri, E., Ihwan, Widodo, A., Nasronudin, & Pitopang, R. (2021). Antioxidant and antiviral potency of Begonia medicinalis fractions. *Journal of Basic and Clinical Physiology and Pharmacology*, *32*(4), 845-851. https://doi.org/10.1515/jbcpp-2020-0435

[12] Khumaidi, A., Widodo, A., Nugrahani, A. W., Sasmito, E., & Fakhrudin, N. (2020). Profil Proliferasi Sel Limfosit Benalu Batu (Begonia medicinalis) Asal Kabupaten Morowali Utara Provinsi Sulawesi Tengah (Lymphocyte Cell Proliferation Profi le of Begonia medicinalis from North Morowali Regency Central Sulawesi Province). *Jurnal Ilmu Kefarmasian Indonesia*, *18*(1), 61–67. https://doi.org/10.33376/ikfi.v18i1.40

[13] Guli, M., Ardiputra, M. A., Pitopang, R., Sari, R., Hatta, M., Prawiro, S. R., ... & Rahmawati, N. D. (2025). The Anticancer Activity of Ethanol Extract of Begonia medicinalis on Colorectal Cancer Rat Model Induced With 7, 12-Dimethylbenz [A] Anthracene. *Journal of Health and Nutrition Research*, *4*(2), 518-526.

[14] Prayong, P., Barusrux, S., & Weerapreeyakul, N. (2008). Cytotoxic activity screening of some indigenous Thai plants. *Fitoterapia*, *79*(7–8), 598–601. https://doi.org/10.1016/j.fitote.2008.06.007

[15] Widiyastuti, Y., Pratiwi, R., Riyanto, S., & Wahyuono, S. (2018). Cytotoxic activity and apoptosis induction of avocado Persea americana Mill. Seed extract on MCF-7 cancer cell line. *Indonesian Journal of Biotechnology*, *23*(2), 61–67. https://doi.org/10.22146/ijbiotech.32141

[16] Dasari, S., & Bernard Tchounwou, P. (2014). Cisplatin in cancer therapy: Molecular mechanisms of action. *European Journal of Pharmacology*, *740*, 364–378. https://doi.org/10.1016/j.ejphar.2014.07.025

[17] Caldwell, G. W., Yan, Z., Lang, W., & Masucci, J. A. (2012). The IC 50 Concept Revisited. *Curr. Top. Med. Chem.*, *12*, 1282–1290. https://doi.org/10.2174/156802612800673327

[18] Nguyen, N. H., Ta, Q. T. H., Pham, Q. T., Luong, T. N. H., Van Trung Phung, T., Duong, H.-H., & Vo, V. G. (2020). Anticancer Activity of Novel Plant Extracts and. *Molecules*, *25*(2912), 1–16. https://doi.org/10.3390/molecules25122912

[19] Da'i, M., Meilinasary, K. A., Suhendi, A., & Haryanti, S. (2019). Selectivity index of alpinia galanga extract and 1'-acetoxychavicol acetate on cancer cell lines. *Indonesian Journal of Cancer Chemoprevention*, *10*(2), 95-100. https://doi.org/10.14499/indonesianjcanchemoprev10iss2pp95-100

[20] Dahham, S. S., Tabana, Y. M., Iqbal, M. A., Ahamed, M. B. K., Ezzat, M. O., Majid, A. S. A., & Majid, A. M. S. A. (2015). The anticancer, antioxidant and antimicrobial properties of the sesquiterpene β-caryophyllene from the essential oil of Aquilaria crassna. *Molecules*, *20*(7), 11808–11829 https://doi.org/10.3390/molecules200711808

[21] Indrayanto, G., Putra, G. S., & Suhud, F. (2021). Validation of in-vitro bioassay methods: Application in herbal drug research. In *Profiles of Drug Substances, Excipients and Related Methodology* (1st ed., Vol. 46). Elsevier Inc. https://doi.org/10.1016/bs.podrm.2020.07.005

[22] Poojar, B., Ommurugan, B., Adiga, S., Thomas, H., Sori, R. K., Poojar, B., Hodlur, N., Tilak, A., Korde, R., Gandigawad, P., In, M., Sleep, R., Albino, D., Rats, W., Article, O., Schedule, P., Injury, C. C., Sori, R. K., Poojar, B., Gandigawad, P. (2017). Methodology Used in the Study. *Asian Journal of Pharmaceutical and Clinical Research*, *7*(10), 1–5.

[23] Maurya, A. (2018). Vacuum Liquid Chromatography: Simple, Efficient and Versatile Separation Technique for Natural Products. *Organic & Medicinal Chemistry International Journal*, *7*(2), 1–3.

[24] Bele, A. A., & Khale., A. (2011). An Overview on Thin Layer Chromatography Archana A. Bele* and Anubha Khale H. K. College of Pharmacy, Jogeshwari (W), Mumbai, Maharashtra, India. *Journal of Pharmaceutical Sciences*, *2*(2), 256–267 https://doi.org/10.19080/OMCIJ.2018.07.555708

[25] Katrin, K., & Bendra, A. (2015). Aktivitas Antioksidan Ekstrak, Fraksi dan Golongan SenyawaKimia Daun Premna oblongata Miq. *Pharmaceutical Sciences and Research*, *2*(1), 21-31. https://doi.org/10.7454/psr.v2i1.3323

[26] Eslaminejad, T., Pourshojaei, Y., Naghizadeh, M., Eslami, H., Daneshpajouh, M., & Hassanzadeh, A. (2022). Synthesis of some benzylidene thiosemicarbazide derivatives and evaluation of their cytotoxicity on U87, MCF-7, A549, 3T3 and HUVEC cell lines. *Journal of the Serbian Chemical Society*, *87*(10), 1125-1142. https://doi.org/10.2298/JSC220203038E

[27] Peña-Morán, O. A., Villarreal, M. L., Álvarez-Berber, L., Meneses-Acosta, A., & Rodríguez-López, V. (2016). Cytotoxicity, post-treatment recovery, and selectivity analysis of naturally occurring podophyllotoxins from Bursera fagaroides var. fagaroides on breast cancer cell lines. *Molecules*, *21*(8), 1013. https://doi.org/10.3390/molecules21081013

[28] Choi, M., Park, S. M., & Cho, K. H. (2022). Evaluating a therapeutic window for precision medicine by integrating genomic profiles and p53 network dynamics. *Communications Biology*, *5*(1), 924. https://doi.org/10.1038/s42003-022-03893-w

[29] Gutbrod, P., Yang, W., Grujicic, G. V., Peisker, H., Gutbrod, K., Du, L. F., & Dörmann, P. (2021). Phytol derived from chlorophyll hydrolysis in plants is metabolized via phytenal. *Journal of Biological Chemistry*, 296, 100530. https://doi.org/10.1016/j.jbc.2021.100530.

[30] Tang, C., Wan, Z., Chen, Y., Tang, Y., Fan, W., Cao, Y., Song, M., Qin, J., Xiao, H., Guo, S., & Tang, Z. (2022). Structure and Properties of Organogels Prepared from Rapeseed Oil with Stigmasterol. *Foods*, *11*(7), 1–14. https://doi.org/10.3390/foods11071001

[31] Aboobucker, S. I., & Suza, W. P. (2019). Why do plants convert sitosterol to stigmasterol?. *Frontiers in plant science*, *10*, 354. https://doi.org/10.3389/fpls.2019.00354

[32] Zhang, X., Wang, J., Zhu, L., Wang, X., Meng, F., Xia, L., & Zhang, H. (2022). Advances in Stigmasterol on its anti-tumor effect and mechanism of action. *Frontiers in oncology*, *12*, 1101289. https://doi.org/10.3389/fonc.2022.1101289

[33] Nazir, S., Chaudhary, W. A., Mobashar, A., Anjum, I., Hameed, S., & Azhar, S. (2023). Campesterol: A Natural Phytochemical with Anti Inflammatory Properties as Potential Therapeutic Agent for Rheumatoid Arthritis: A Systematic Review. *Pakistan Journal of Health Sciences*

[34] Bae, H., Park, S., Yang, C., Song, G., & Lim, W. (2021). Disruption of endoplasmic reticulum and ROS production in human ovarian cancer by campesterol. *Antioxidants*, *10*(3), 379. https://doi.org/10.3390/antiox10030379

[35] Altaf, A., Maqbool, T., Hassan, A., Nasreen, G., Summan, M., Tahir, A., ... & Koser, N. Campesterol induces apoptosis and inhibits proliferation in HepG2 liver cancer cells. *Clinical and Experimental Hepatology*, *11*(1).

[36] Dias, V., Uqueio, M., Nhaca, A., & Salência, H. (2020). Qualitative Analysis of Phytocompounds of Liagora divaricata and Trematocarpus flabellatus. *Journal of Drug Delivery and Therapeutics*, *10*(5), 75–81 https://doi.org/10.22270/jddt.v10i5.4367

[37] Selmy, A. H., Hegazy, M. M., El-Hela, A. A., Saleh, A. M., & El-Hamouly, M. M. (2023). In Vitroand in Silico studies of Neophytadiene; A Diterpene Isolated Fromaeschynomene Elaphroxylon (Guill. &Perr.) Taub. as Apoptotic Inducer. *Egyptian Journal of Chemistry*, *66*(10), 149-161. https://doi.org/10.21608/ejchem.2023.180252.7314

[38] De-Eknamkul, W., & Potduang, B. (2003). Biosynthesis of β-sitosterol and stigmasterol in Croton sublyratus proceeds via a mixed origin of isoprene units. *Phytochemistry*, *62*(3), 389-398

[39] Shahbaz, M., Momal, U., Perween, A., Naeem, H., Hussain, M., Imran, M., ... & Mohamed, H. M. (2026). Anticancer Molecular Mechanisms of Phytosterols: An Updated Review on Clinical Trials. *Food Science & Nutrition*, *14*(2), e71505.

[40] Senbagalakshmi, P., Muthukrishnan, T., Jebasingh, T., Senthil Kumar, T., & Rao, M. V. (2019). Squalene, biosynthesis and its role in production of bioactive compounds, a proper scientific challenge - A review. *Journal of Emerging Technologies and Innovative Research*, *6*(2), 505–526.

[41] Bidooki, S. H., Quero, J., Sánchez-Marco, J., Herrero-Continente, T., Marmol, I., Lasheras, R., ... & Rodriguez-Yoldi, M. J. (2024). Squalene in Nanoparticles Improves Antiproliferative Effect on Human Colon Carcinoma Cells Through Apoptosis by Disturbances in Redox Balance. *International Journal of Molecular Sciences*, *25*(23), 13048. https://doi.org/10.3390/ijms252313048

[42] Gutbrod, P., Yang, W., Grujicic, G. V., Peisker, H., Gutbrod, K., Du, L. F., & Dörmann, P. (2021). Phytol derived from chlorophyll hydrolysis in plants is metabolized via phytenal. *Journal of Biological Chemistry*, *296*, 100530.

[43] Sakthivel, R., Malar, D. S., & Devi, K. P. (2018). Phytol shows anti-angiogenic activity and induces apoptosis in A549 cells by depolarizing the mitochondrial membrane potential. *Biomedicine & Pharmacotherapy*, *105*, 742-752. https://doi.org/10.1016/j.biopha.2018.06.040

[44] Boadu, A., Karpoormath, R., & Nlooto, M. (2024). Spondias mombin: biosafety and GC–MS analysis of anti-viral compounds from crude leaf extracts. *Advances in Traditional Medicine*, *24*(1), 349–372. https://doi.org/10.1007/s13596-023-00685-9

[45] Arora, S., & Meena, S. (2017). GC-MS Profiling of Ceropegia bulbosa Roxb. var. bulbosa, an endangered plant from Thar Desert, Rajasthan. *Pharma Innov J*, *6*(11), 568-573.

[46] Sunarić, S., Lalić, J., & Spasić, A. (2017). Simultaneous Determination of Alpha-Tocopherol and Alpha-Tocopheryl Acetate in Dairy Products, Plant Milks and Health Supplements by Using SPE and HPLC Method. *Food Analytical Methods*, *10*(12), 3886–3901. https://doi.org/10.1007/s12161-017-0953-3

[47] Ali, H. M., Attia, M. H., Mamdouh, W., Rashed, E. N., & Ali, I. H. (2025). Oxidative degradation of alpha-tocopherol by reactive oxygen species, identifying products, and product anticancer activity. *BMC chemistry*, *19*(1), 306.

[48] Abdullahi, M., & Adeniji, S. E. (2020). In-silico Molecular Docking and ADME/Pharmacokinetic Prediction Studies of Some Novel Carboxamide Derivatives as Anti-tubercular Agents. *Chemistry Africa*, *3*(4), 989–1000 https://doi.org/10.1007/s42250-020-00171-w

[49] Pattanayak, P. (2022). SwissADME Predictions of Drug-Likeness of 5-Nitro Imidazole Derivatives as Potential Antimicrobial and Antifungal Agents. *Russian Journal of Bioorganic Chemistry*, *48*(5), 949–957. https://doi.org/10.1134/S106816202205018X

[50] Ivanović, V., Rančić, M., Arsić, B., & Pavlović, A. (2020). Lipinski's rule of five, famous extensions and famous exceptions. *Chemia Naissensis*, *3*(1), 171–181

[51] Schweiker, S. S., & Levonis, S. M. (2020). Navigating the intricacies of molecular docking. *Future Medicinal Chemistry*, *12*(6), 469–471. https://doi.org/10.4155/fmc-2019-0335

[52] Yusuf, D., Davis, A. M., Kleywegt, G. J., & Schmitt, S. (2008). An alternative method for the evaluation of docking performance: RSR vs RMSD. *Journal of Chemical Information and Modeling*, *48*(7), 1411–1422. https://doi.org/10.1021/ci800084x

[53] Tamirat, M. Z., Kurppa, K. J., Elenius, K., & Johnson, M. S. (2021). Structural basis for the functional changes by EGFR exon 20 insertion mutations. *Cancers*, *13*(5), 1–21. https://doi.org/10.3390/cancers13051146

[54] Bello, M. (2018). Binding mechanism of kinase inhibitors to EGFR and T790M, L858R and L858R/T790M mutants through structural and energetic analysis. *International Journal of Biological Macromolecules*, *118*, 1948–1962. https://doi.org/10.1016/j.ijbiomac.2018.07.054

[55] Li, Z., Jiang, J., Ficarro, S. B., Beyett, T. S., To, C., Tavares, I., Zhu, Y., Li, J., Eck, M. J., Jänne, P. A., Marto, J. A., Zhang, T., Che, J., & Gray, N. S. (2024). Molecular Bidents with Two Electrophilic Warheads as a New Pharmacological Modality. *ACS Central Science*, *10*(6), 1156–1166. https://doi.org/10.1021/acscentsci.4c00222

[56] Truong, T. H., Ung, P. M. U., Palde, P. B., Paulsen, C. E., Schlessinger, A., & Carroll, K. S. (2016). Molecular Basis for Redox Activation of Epidermal Growth Factor Receptor Kinase. *Cell Chemical Biology*, *23*(7), 837–848 https://doi.org/10.1016/j.chembiol.2016.06.006

[57] Nie, W., Tang, L., Zhang, H., Shao, J., Wang, Y., Chen, L., Li, D., & Guan, X. (2012). Structural analysis of the EGFR TK domain and potential implications for EGFR targeted therapy. *International Journal of Oncology*, *40*(6), 1763–1769. https://doi.org/10.3892/ijo.2012.1384

[58] Pandey, Pankaja, Priyanka Joshi, Shilpi Rawat, and Subhash Chandra. 2024. “Computational Analysis Identifies Withastramonolide and Kaempferol as Highly Potent Compounds from Datura Stramonium Targeting EGFR-TK in Non-Small Cell Lung Cancer (NSCLC).” 9(10): 1–7. https://doi.org/10.33263/BRIAC143.030

[59] Yonar, D., Baba, B., & Karayel, A. (2023). Evaluation of zerumbone as an egfr tyrosine kinase inhibitor by molecular docking method. *Journal of Faculty of Pharmacy of Ankara University*, *47*(1), 196-207. https://doi.org/10.33483/jfpau.1171442

[60] Danjolli-Hashani, D., Isbilir, S. S., & Yılmaz, A. Ş. (2025). Punica granatum L. Peel: Anticancer Activity on Hep3B, Drug-likeness, ADMET Prediction, and Molecular Docking with EGFR-TK. *ChemistrySelect*, *10*(3), e202403976

[61] Sora, V., & Papaleo, E. (2022). Structural Details of BH3 Motifs and BH3-Mediated Interactions: an Updated Perspective. *Frontiers in Molecular Biosciences*, *9*(May), 1–20. https://doi.org/10.3389/fmolb.2022.904329

[62] Chen, Y., Wang, J., Zhang, J., & Wang, W. (2018). Binding modes of Bcl-2 homology 3 (BH3) peptides with anti-apoptotic protein A1 and redesign of peptide inhibitors: a computational study. *Journal of Biomolecular Structure and Dynamics*, *36*(15), 3967–3977. https://doi.org/10.1080/07391102.2017.1406859

[63] Gyebi, G., M. Ogunyemi, O., M. Ibrahim, I., O. Afolabi, S., J. Ojo, R., D.I. Ejike, U., & O. Adebayo, J. (2022). Inhibitory potentials of phytocompounds from Ocimum gratissimum against anti-apoptotic BCL-2 proteins associated with cancer: an integrated computational study. *Egyptian Journal of Basic and Applied Sciences*, *9*(1), 588–608. https://doi.org/10.1080/2314808X.2022.2120023

[64] Abd Ghani, M. F., Othman, R., & Nordin, N. (2020). Molecular docking study of naturally derived flavonoids with antiapoptotic BCL-2 and BCL-XL proteins toward ovarian cancer treatment. *Journal of Pharmacy and Bioallied Sciences*, *12*(Suppl 2), S676-S680. https://doi.org/10.4103/jpbs.JPBS_166_20

[65] Gowtham, H. G., Ahmed, F., Anandan, S., Shivakumara, C. S., Bilagi, A., Pradeep, S., ... & Kollur, S. P. (2023). In silico computational studies of bioactive secondary metabolites from Wedelia trilobata against anti-apoptotic B-cell lymphoma-2 (Bcl-2) protein associated with cancer cell survival and resistance. *Molecules*, *28*(4), 1588. https://doi.org/10.3390/molecules28041588